Reports

The Structure of the Core of the Spiral Wave in the Belousov-Zhabotinskii Reaction

Abstract. *The quantitative structure of the core of the spiral-shaped traveling wave of chemical activity appearing in a thin excitable layer of the Belousov-Zhabotinskii reaction, in which the oxidation and decarboxylation of malonic acid by bromate ions is catalyzed by ferroin, was analyzed experimentally. Light absorption by ferroin as the reduced reaction catalyst and indicator was measured by means of a video- and computer-based two-dimensional spectrophotometer with 10-micrometer spatial, 2-second temporal, and 256–digital units intensity resolution. The spiral core is a singular site (diameter, 30 micrometers or less) at which intensity modulations due to ferroin-ferriin distributions are at least ten times smaller than in the surrounding area of spiral propagation. Archimedian spirals were fitted to isoconcentration lines.*

STEFAN C. MÜLLER
THEO PLESSER
BENNO HESS
Max-Planck-Institut für Ernährungsphysiologie, Rheinlanddamm 201, D-4600 Dortmund, Federal Republic of Germany

The formation of spatial patterns in chemical systems resulting from the coupling of reaction with transport processes such as diffusion or convection has been extensively studied, both theoretically and experimentally, during the past decade (*1*). The Belousov-Zhabotinskii (BZ) reaction has received considerable attention as an example of chemical wave propagation (*1–3*). Detailed experiments on chemical aspects have been reported (*4*), but quantitative data on the geometric and kinematic properties of the waves have been rare (*3, 5*). A recent investigation yielded quantitative descriptions of concentric waves in terms of concentration distributions by recording absorption on a one-dimensional photodiode array (*6*). However, theoretical models of chemical waves have been developed that require more experimental details for their support (*7*).

We now describe our two-dimensional (2D) study of spiral patterns formed in a thin layer of the BZ reaction system, with emphasis on the spatial distribution of the catalyst (ferroin) concentration within and close to the core region. Measurements were carried out with a 2D spectrophotometer based on a TV camera linked to a computer system. The spiral core is a singular site at which variations in ferroin and ferriin concentrations are at least ten times smaller than the modulations of large amplitude that occur at all other sites in the surrounding area. The observations facilitated the comparison of calculated spirals with the corresponding measured ferroin concentrations.

A quiescent but excitable BZ system was obtained by preparing a reactive mixture of 48 m*M* NaBr, 340 m*M* $NaBrO_3$, 95 m*M* $CH_2(COOH)_2$, and 378 m*M* H_2SO_4 in a final volume of 5 ml. About 5 minutes later, 3.5 m*M* ferroin was added to the solution. Distilled water and reagent-grade chemicals were used. After filtering through a 0.44-μm Millipore filter, 3.6 ml of the mixture was placed in a siliconized, dust-free petri dish (diameter, 6.8 cm) at 24° ± 1°C. A concentric wave was triggered by immersing the tip of a hot (≈200°C) platinum wire (diameter, 0.3 mm) into the solution layer (depth, 1 mm) for 0.5 second. After the diameter of the propagating circular wave had reached 1 cm, a spiral wave was initiated by disrupting a small section of the wave front with a gentle blast of air ejected from a 500-μl Eppendorf pipette. Immediately afterward, the dish was covered with a glass plate (leaving an air gap 12 mm in height), thus preventing the formation of convective patterns by evaporative cooling of the layer surface (*8*).

The light absorption of the evolving spiral was measured by 2D photometric techniques. The sample layer was illuminated by a parallel light field with a spatial homogeneity better than ±1.5 percent per centimeter. The wavelength of maximum ferroin and minimum ferriin absorption (490 nm) was selected by an interference filter of 10-nm bandwidth. A square section of the object plane (5 by 5 mm^2) was imaged on the 2D intensity detector, which was comprised of a TV camera system (Hamamatsu C1000) equipped with a Vidicon tube (Hamamatsu N983) having an image raster resolution of 512 by 512 picture elements (pixels) and an intensity resolution of 256 digital units. Quantitative acquisition and digital storage of 2D transmission data on magnetic disk was feasible at a frequency up to 30 frames per minute by combining the camera with a video frame buffer (VTE, Digitalvideo GmbH, Braunschweig) and a computer (Perkin-

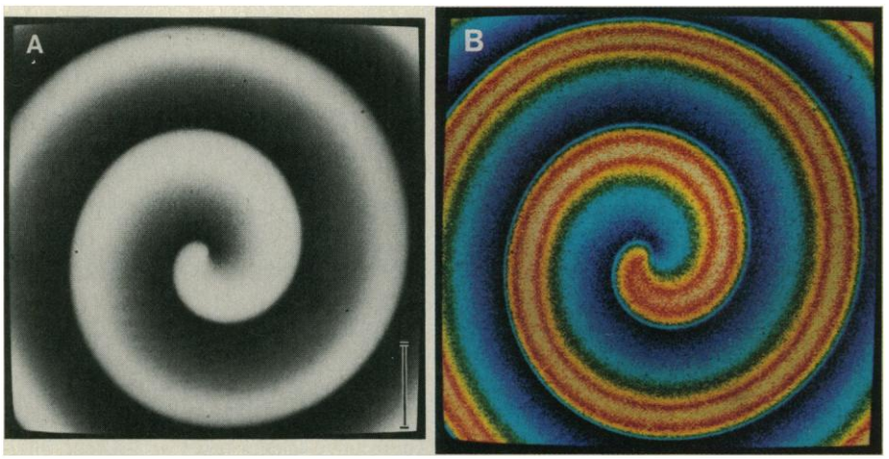

Fig. 1. Digital image of a spiral wave propagating in a 1-mm layer of an excitable Belousov-Zhabotinskii reagent observed at 490 nm 5 minutes after placing the solution in a petri dish and 2 minutes after initiating the spiral pattern. The snapshot shows a 4.5 by 4.5 mm^2 section of the dish. Seven intensity intervals of equal width in (A) are represented by pseudocolors in (B) and indicate in some detail the geometric features of specific levels of transmitted light intensity, which correspond to isoconcentration lines of the dye ferroin. Scale bar, 1 mm.

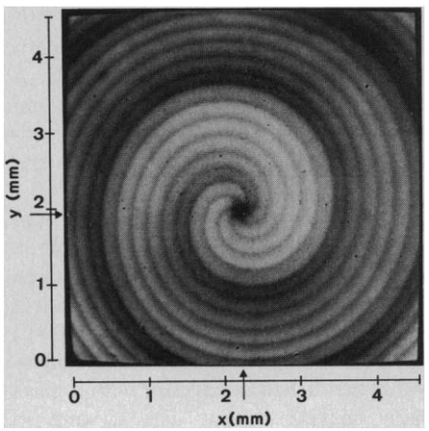

Fig. 2 (left). Additive composition of transmitted light intensities of six digital images of the propagating spiral wave. The images were taken at 3-second intervals (including the image in Fig. 1) and cover almost precisely one revolution of the spiral. The dark spot centered at $x_0 = 2.25$ mm, $y_0 = 1.95$ mm (arrows) indicates a circular region around the core of the spiral, in which temporal modulations of light intensity are distinctively lower than in the surrounding area.

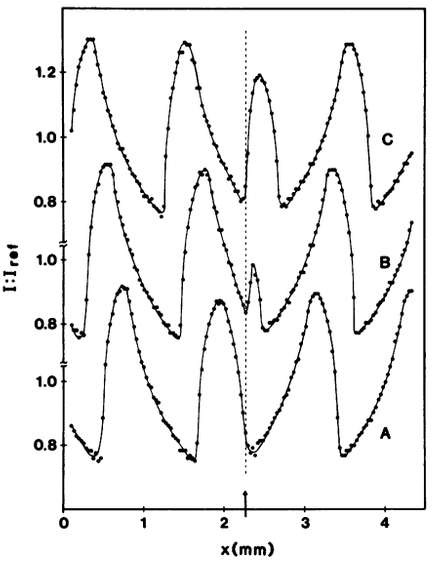

Fig. 3 (right). Intensity profiles plotted against the x coordinate passing through the spiral core (see Fig. 2). Profile A was obtained from Fig. 1, and profiles B and C were obtained from images taken 3 and 6 seconds later, respectively. For better illustration of the continuity of the curves, solid lines were drawn by hand to fit the measured points. The x coordinate of the core is marked by the vertical dashed line and the arrow. The intensities at the core remained approximately steady. The shape of the waves is highly asymmetric outside the core region.

Elmer 3230) with a 4-megabyte main memory. Software routines were available for corrections of temporal and spatial background inhomogeneities, for reduction of pixel noise, and for further evaluation of image data (*9*).

A 450 by 450 pixel image of the spiral was photographed from a black and white TV screen (Fig. 1A) and, in a pseudocolor representation, from a color monitor (Fig. 1B) 2 minutes after spiral initiation (*10*). Consecutive images were stored at 3-second intervals during the subsequent observation period of 2 minutes. The intensity I in these images is modulated in space with respect to their average intensity I_{ref} in the range $0.75 \leq I:I_{ref} \leq 1.3$. A composite image of six additively superposed, consecutive frames is shown in Fig. 2. Since the revolution period of the clockwise inward-turning tip of the spiral (whereby the wave fronts move outward) amounted to 17.4 seconds, the image covers about one revolution. Each of the six bands is predominantly determined by the intensity "crest" of the spiral pattern in the corresponding original image. They all merge into a dark region in the center of the picture, which contains the core of the rotating spiral wave. In this region the light intensity always remains distinctly below the levels measured in the vicinity of the bright spiral crest, which moves through all outer areas. The coordinates of the center (arrows, Fig. 2) were estimated to be $x_0 = 2.25$ mm, $y_0 = 1.95$ mm.

The core region was further analyzed by extracting intensity profiles from the stored image data. In Fig. 3 three profiles are shown that were obtained at intervals of 3 seconds along the horizontal line where $y = y_0$. In this sequence, the cross-section of the revolving bright spiral tip appeared close to the right of the core. In profile A it is only barely recognizable because of the scattering of data points, whereas in profile B, 3 seconds after the tip crossed the line along which the profiles were taken, a small but distinct intensity peak has emerged. In profile C the peak has almost grown to the height of the wave crest in the outer area to the left and right. However, it has not yet assumed the asymmetric shape that is characteristic of the waves with intensity peaks at distances from the core larger than 0.7 mm.

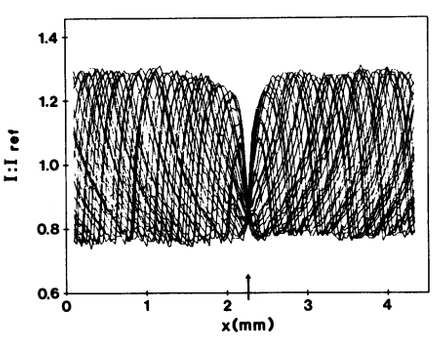

Fig. 4. Superposition of 26 intensity profiles such as shown in Fig. 3, calculated from consecutive images taken at 3-second intervals (including Fig. 1) covering more than four spiral revolutions. The intensity units of the ordinate are identical with those of Fig. 3. At the core of the spiral (arrow), the intensity modulation is less than 10 percent of the full amplitude of the wave moving through all other sites during its outward displacement.

The intensities measured at the core location in Fig. 3 were approximately constant ($I \approx 0.86\ I_{ref}$). This finding is illustrated in Fig. 4, in which 26 intensity profiles along the same line as in Fig. 3 are directly superposed. This representation yields more details about the properties of the spiral core at $x_0 = 2.25$ mm (arrow; compare with Fig. 2). Its outstanding singular feature is that, in its very center, the intensity variation remains below 10 percent of that of the full wave amplitude. With a diameter of 30 μm or less, the core center occupies a volume smaller than 7×10^{-7} ml. There is a larger region with a diameter of about 700 μm in which the medium is never excited to full ferroin or ferriin amplitudes, as is the case in the outside area. This finding suggests a local predominance of one of the three main reaction steps of the BZ reaction (*4*) in a volume of about 4×10^{-4} ml. The average intensity level at the center of the core is maintained at 0.86 I_{ref}, a value close to but above the minimum level at 0.75 I_{ref}.

An analysis of the geometric characteristics of the spiral wave is presented in the cover picture. The picture consists of the black-and-white image of Fig. 1A and of colored Archimedian spirals superposed on the image by digital techniques. These were calculated by fitting the parameters a and φ_0 of the spiral equation in polar coordinates, $r = a(\varphi - \varphi_0)$, to selected isointensity lines. As a first obvious approach, the curves present an adequate description of the observed geometry. The cartesian coordinates of the spiral origin as derived from the fit to the intensity of the wave crest (red spiral in the cover picture) are $x_0 = 2.26$ mm and $y_0 = 1.98$ mm, which are in good agreement with the local estimate of the coordinates for the center of the core (Figs. 2 and 4). From similar fits for consecutive images, a set of φ_0 values is obtained that results in a revolution period of 17.4 seconds. The period and the precisely determined spiral parameter $a = 190$ μm yield a wave propagation velocity of 69 μm sec^{-1}, which is in the range given previously (*5*). These numbers remained valid for the more than six revolutions that occurred during our observation period. The green circle in the cover pic-

ture encloses the center of the core and its immediate surroundings. In this region, of course, the simple spiral representation of isointensity lines is not applicable.

Our experimental evidence for the existence and the structure of the core of the spiral pattern exhibited in the BZ reaction system shows the importance of a locally restricted phenomenon driving and controlling the spiral propagation through space. Our observation shows the stable coexistence of two different dynamic states in space. Further application of the digital video technique for a quantitative description of the dynamic behavior of the core and the local predominance of specific reaction steps at its center is expected to lead to stimulating contributions to our knowledge of chemical waves. Furthermore, the spatial transition from the local to the bulk state in terms of the outward moving chemical activity is of utmost interest.

References and Notes

1. C. Vidal and A. Pacault, Eds., *Springer Ser. Synerget.* **27**, 1 (1984). See also vols. 6, 12, 19, and 28 in this series.
2. H.-G. Busse, *J. Phys. Chem.* **73**, 750 (1969); A. N. Zaikin and A. M. Zhabotinskii, *Nature (London)* **225**, 535 (1970); H.-G. Busse and B. Hess, *ibid.* **244**, 203 (1973).
3. A. T. Winfree, *Science* **175**, 634 (1972); *Sci. Am.* **230**, 82 (June 1974).
4. R. J. Field, E. Körös, R. M. Noyes, *J. Am. Chem. Soc.* **94**, 8649 (1972); L. Bornmann, H.-G. Busse, B. Hess, *Z. Naturforsch. Teil B* **28**, 93 (1973); *Z. Naturforsch. Teil C* **28**, 514 (1973); L. Bornmann *et al.*, *Z. Naturforsch. Teil B* **28**, 824 (1973).
5. K. Showalter, R. M. Noyes, H. Turner, *J. Am. Chem. Soc.* **101**, 7463 (1979); M. L. Smoes, *Springer Ser. Synerget.* **6**, 80 (1980).
6. P. M. Wood and J. Ross, *J. Chem. Phys.* **82**, 1924 (1985).
7. P. Ortoleva and J. Ross, *ibid.* **58**, 5673 (1973); J. J. Tyson, *Lect. Notes Biomath.* **10**, 1 (1976); P. C. Fife, NATO *Adv. Study Inst. Ser. B* **116**, 371 (1984).
8. S. C. Müller and T. Plesser, *Lect. Notes Biomath.* **55**, 246 (1984).
9. ———, B. Hess, *Anal. Biochem.* **146**, 125 (1985).
10. Because of the curvature of the TV observation screen, the geometry of the photographs in Figs. 1, 2, and on the cover is slightly distorted.

11. We thank K. Dreher, U. Heidecke, B. Plettenberg, R. Schüller, and G. Schulte for skillful technical and programming support.

23 April 1985; accepted 12 July 1985

Intracellular Free Calcium Localization in Neutrophils During Phagocytosis

Abstract. *Intracellular free calcium ($Ca^{2+}{}_i$) is thought to be an important second messenger for phagocyte functions. The fluorescent indicator Quin2 was used to measure and visualize $[Ca^{2+}]_i$ in human neutrophils during chemotaxis toward, and phagocytosis of, opsonized zymosan. In neutrophils migrating toward zymosan, $[Ca^{2+}]_i$ was highest in the lamellipodium. Neutrophils ingesting opsonized zymosan had the highest $[Ca^{2+}]_i$ in the pseudopods and periphagosomal cytoplasm. Most of the increase in $[Ca^{2+}]_i$ was from extracellular sources. Regional increments in $[Ca^{2+}]_i$ are strategically located to modulate such cellular functions as chemotaxis, oxidative activity, and degranulation.*

DANIEL W. SAWYER
JAMES A. SULLIVAN
GERALD L. MANDELL*
Division of Infectious Diseases, Department of Internal Medicine, University of Virginia School of Medicine, Charlottesville 22908

* To whom correspondence should be addressed.

Intracellular free calcium ($Ca^{2+}{}_i$) is thought to be an important secondary messenger for many phagocyte functions including chemotaxis (*1*), phagocytosis (*2*), and degranulation (*3*). Surface stimuli trigger transient changes in calcium concentration that are associated with these effector functions. The subcellular pattern of Ca^{2+} distribution in resting and stimulated neutrophils is largely unknown because in prior studies changes in populations of cells were analyzed with fluorometric or photometric techniques. We investigated the alterations in the subcellular distribution of Ca^{2+} in neutrophils during chemotaxis and phagocytosis with the Ca^{2+} indicator Quin2. This indicator emits Ca^{2+}-dependent fluorescence when excited at 340 nm and Ca^{2+}-independent fluorescence when excited at 360 nm (*4*).

Neutrophils were isolated from heparinized (10 units per milliliter) venous blood of normal volunteers by Ficoll-Hypaque separation (*5*); after isolation, the neutrophils were subjected to dextran sedimentation and hypotonic lysis of erythrocytes. Isolated neutrophils were washed with Hanks balanced salt solution (HBSS) and loaded with 25 μM Quin2 ester (Calbiochem) for 60 minutes at 37°C. The cells were washed with HBSS plus 1 percent autologous heat-inactivated serum and incubated at 24°C for 120 minutes, allowing hydrolysis of the ester to the active Ca^{2+} indicator. For experiments without extracellular calcium ($[Ca^{2+}]_0$), the Quin2-loaded cells were spun and resuspended in Ca^{2+}- and Mg^{2+}-free HBSS with 10 mM EGTA.

Quin2-loaded neutrophils (10^6 cells per milliliter) were transferred to a cover glass, mixed with opsonized zymosan (*6*), and observed with a microscope (Leitz Orthoplan) equipped with a 100-W mercury vapor epi-illuminator, quartz optical elements in the epifluorescence pathway, and a glycerine immersion objective (Nikon 100× UV-CF). Neutrophils for analysis were selected with bright-field microscopy. Images of Quin2-loaded neutrophils were collected with a silicon-intensified target camera (DAGE series 65) and stored for later processing with an image processor (Quantex 9210). Three images of single cells were collected in sequence over less than 5 seconds. The first image was a processed bright-field image based on the use of a modification of asymmetric illumination contrast optics (*7*), in which a circular filter (50 mm in diameter), one half clear and one half black, was placed in the transmitted light path. Processing included the averaging of eight frames, background subtraction, and gray-scale expansion. This image was used to establish the location of morphological features. The second and third images were fluorescence images obtained with a long-pass barrier filter that transmits wavelengths >475 nm. Cells were excited first at 340 nm (10-nm half width) and subsequently at 360 nm (10-nm half width paired with a .25 percent transmission neutral density filter). Each of the fluorescence images was an average of eight video frames. The two fluorescence images were separated in time by less than 0.5 second.

To determine $[Ca^{2+}]_i$, we first converted each raw fluorescence image to a pixel array (640 by 480 by 8 bits). Point density readings were taken first within the 360-nm fluorescence image, and then at the corresponding pixels within the 340-nm fluorescence image. The ratio of the fluorescence intensity at 340 nm to that at 360 nm, when applied to a curve relating known concentrations of Ca^{2+} (*8*, *9*), indicated the $[Ca^{2+}]_i$ at that point in the cell. We did not detect neutrophil autofluorescence with this system.

To visually display the relative local $[Ca^{2+}]_i$ within a single cell, we converted the intensity of each pixel of the two digitized fluorescence images to a logarithm and subtracted the 360-nm log image from the 340-nm log image. The antilog of the difference represents the free Ca^{2+} distribution and is independent of Quin2 concentrations at specific image locations.

Measurements of $[Ca^{2+}]_i$ in unstimulated but polarized neutrophils are listed in Table 1A. The mean $[Ca^{2+}]_i$ in the